Article
Vol. 26, No. 4, p. 487–498, August 2022
https://doi.org/10.1007/s12303-022-0002-5
pISSN 1226-4806 eISSN 1598-7477
Geosciences Journal GJ

Multiple and single grain quartz OSL dating of dolmens in Jungdo, central Korean Peninsula

Seok-Jin Kim[1,2], Jeong-Heon Choi[1]*, Hyoun Soo Lim[2], Seungwon Shin[3], Eun-Young Yeo[4], Hyo-Jeong Weon[1,3], and Seoyoung Heo[4]

[1]Research Center for Geochronology and Isotope Analysis, Korea Basic Science Institute, Chungbuk 28119, Republic of Korea
[2]Department of Geological Sciences, Pusan National University, Busan 46241, Republic of Korea
[3]Division of Geology and Geophysics, Kangwon National University, Chuncheon 24341, Republic of Korea
[4]Center for Research Equipment, Korea Basic Science Institute, Chungbuk 28119, Republic of Korea

ABSTRACT: In the last few years, substantial amount of archaeological remains, which belong to the Bronze and the Iron Ages, has been excavated in Jungdo, central part of Korean peninsula, indicating that the prehistoric (partly, early historic) cultures had been flourished in this area. Particularly, more than 150 dolmens were found during the excavation campaign, and they have drawn keen attentions because dolmens are controversially regarded as being the representative remains for the Bronze Age in Korean peninsula. Despite their archaeological importance for understanding the ancient cultural and social aspects in Korean peninsula, the chronology of the dolmens has largely been dependent upon sensory tests using concomitant artifacts while numerical dating has been scarce and limited to the case when organic materials for radiocarbon dating were available. Recent advances in luminescence dating, however, allow direct dating of stone structures, like dolmens, by measuring OSL (Optically Stimulated Luminescence) signals in phosphor minerals underneath the stone structures. In this paper, we performed OSL dating of quartz collected from underneath the stones making up dolmens in Jungdo. For OSL dating, we chose three dolmens and six sediment samples were collected from them. Using multiple grain aliquots, consisting of ~300 quartz grains, the OSL ages of ~4.3–3.2 ka were obtained. These ages, however, appear to be older than previously reported radiocarbon ages in Jungdo and a radiocarbon age (2119–1750 cal yr BP) of a human bone sample excavated from one of the dolmens. On the contrary, single grain OSL dating yielded MAM-3 (Minimum Age Model with three parameters) ages consistent with the radiocarbon age, ranging ~2.9–2.2 ka. Our results suggest that Jungdo has been the place either for burial plots or habitation of the ancient humans up to early Iron Age in the central part of Korean peninsula.

Key words: dolmen, Jungdo, multiple grain aliquot, single grain, quartz OSL, age model

Manuscript received September 8, 2021; Manuscript accepted January 14, 2022

1. INTRODUCTION

Megalithic remains have been reported from many countries in Europe, Africa, Asia and others (Wright, 2007; Kostov, 2008; Laporte et al., 2012; Nelson, 2014; Bae and Kim, 2015; Nesterkina et al., 2017; Sharon et al., 2017). In general, megalithic remains are associated with structures which consist of large rocks or carved stones by ancient humans with the purpose of worship or ancient grave usage etc. Therefore, to establish reliable chronology of these prehistoric structures is crucial for understanding the social and cultural aspects of ancient humans who built them (Kostov, 2008; Ko, 2009; Laporte et al., 2012; Bae and Kim, 2015; Nesterkina et al., 2017).

Recently, OSL (Optically Stimulated Luminescence) dating method, which is conventionally used for dating unconsolidated Quaternary sediments, has successfully been applied to dating stone structures with archaeological significance. One of the earliest attempts is the rock surface dating on a medieval castle in Germany and the Nazca lines in Peru by Greilich et al. (2005). In this work, using the OSL signals from quartz and feldspars in rock slices (without mineral separation) taken from the surface of rocks that had been exposed to sunlight during construction and destruction, they obtained the OSL ages consistent with historical and archaeological evidences. Athanassas et al. (2015) performed quartz OSL dating of prehistoric stone structures

***Corresponding author:**
Jeong-Heon Choi
Research Center for Geochronology and Isotope Analysis, Korea Basic Science Institute, 162 Yeongudanji-ro, Cheongwon-gu, Cheongju, Chungbuk 28119, Republic of Korea
Tel: +82-43-240-5333, Fax: +82-43-240-5179, E-mail: jhchoi@kbsi.re.kr

observed at Wadi Wisad, northern Arabian Desert, using sediments underneath the basaltic rocks (these were called "slabs" by the authors), and showed that their OSL ages were in good agreement with the previous radiocarbon ages on charcoals from the settlement site of Wisad Pools, Jordan. These authors later carried out quartz OSL dating on dolmens in Spain (Athanassas et al., 2017). Quartz grains used for OSL dating in this study were chemically extracted from cobble surface, assuming that the OSL signals in surficial quartz might have been well bleached by sunlight exposure during construction of the dolmens. In addition, quartz from mud adhering the cobbles were also OSL dated for their investigation. While most of their samples yielded archaeologically reasonable OSL ages, for some samples, the OSL ages of quartz from both cobble surface and adhering mud were observed to be older than those expected from archaeological contexts, which were attributed to the influence of incompletely bleached grains.

Among other megalithic structures, dolmens, the ancient stone grave structures, provide important archaeological clues for understanding the characteristics of ancient society and cultures because dolmens may contain various types of archaeological remains, together with ancient human bones. From many places in Korean peninsula, a large number of dolmens have long been excavated and reported (e.g., Kim, 2015); Dolmens are regarded as being the archaeological remains representative of the Bronze age in Korean peninsula. Particularly, over the last few decades, there have been intensive archaeological excavations in Jungdo, the central part of Korean peninsula (Fig. 1). Through the excavation campaign, a significant number of dolmens have been reported, along with the archaeological remains representing the Neolithic to early Iron age. However, the numerical ages that are directly relevant to the construction timing of the dolmens are scant, except the case when organic materials (human bones and charcoals) for radiocarbon dating were available (e.g., Rhee and Choi, 1992; Kang, 2010).

In this paper, we investigated the possibility of applying OSL dating method to dolmens in Jungdo, using multiple and single grains of quartz recovered from the surface of fluvial sediments underneath the stones making up the dolmens. We also examined the OSL ages derived by central and minimum age models (Galbraith et al., 1999), in order to see which age model is appropriate to be applied for OSL dating of the dolmens in Jungdo. Finally, we suggested the construction timing of the dolmens in Jungdo using the OSL dating method for the first time in Korean peninsula.

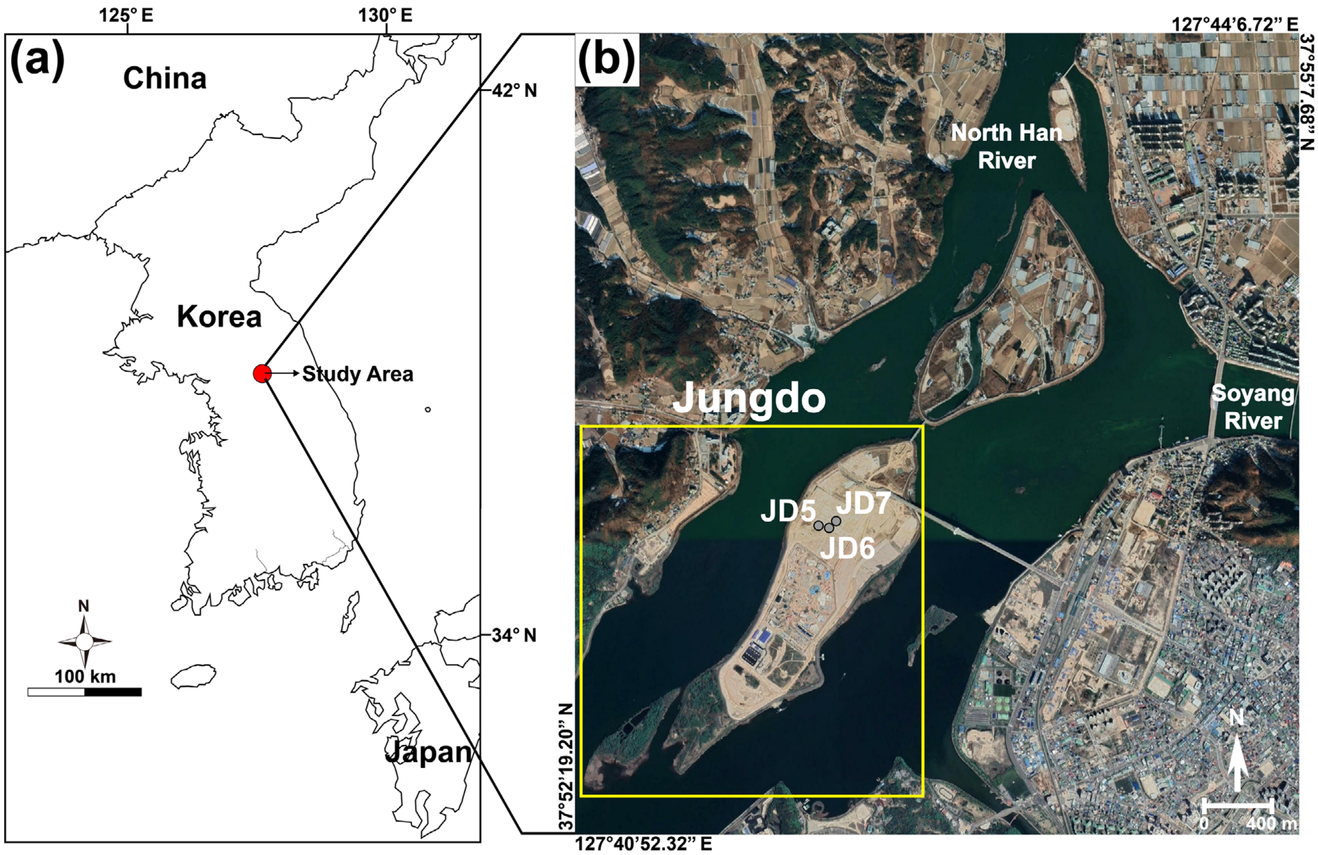

Fig. 1. The study area and sampling sites. (a) Jungdo, the study area, is located at the central part of Korean peninsula and (b) three dolmens (JD5, JD6 and JD7) were chosen for the investigation.

2. STUDY AREA AND SAMPLE DETAILS

Jungdo is a river island, located at the junction of the North Han river and the Soyang river, in the central part of the Korean peninsula (Fig. 1). This island is considered to have formed by episodic deposition of fluvial sediments during the Holocene period; The detailed sedimentological and geochronological investigations on Jungdo will be dealt with elsewhere by the present authors.

Dolmens were constructed by putting stones of various sizes (approx. ~20 to 50 cm) rectangularly or ovally on the ground (Fig. 2). Stones making up the dolmens in the study area are mainly composed of granite, gneiss and quartzite, presumably collected from the vicinity, and these are put on the surface of fluvial sediments. Thus, it is highly probable that quartz grains at the sediment surface, immediately below the stones, have been exposed to sunlight for prolonged time enough for the OSL signals to be sufficiently reset. If this is the case, the OSL ages of quartz grains should indicate the time elapsed since the stones have been laid down to construct dolmens. To test this hypothesis, we chose three representative dolmens (JD5, 6 and 7; Fig. 1b), and the samples were taken for OSL dating from the topmost sediments (down to ~1 cm in depth), immediately underneath the stones of each dolmen (Fig. 2d); Chapot et al. (2012) suggested that, considering the possibility of incorporation of quartz grains irrelevant to archaeological event into sediments, the OSL ages using quartz recovered from surface of the stones should be more reliable than those of underlying sediments. However, due to the Korean Cultural Heritage Protection Law, we could not collect stones from the dolmens in Jungdo.

Sample collections were carried out at night to prevent quartz grains from being exposed to sunlight during sampling. As shown in Figure 2, it is observed that, for the dolmens JD 6 and 7, one group of stones are buried in the inner part, and the others are on the exposed surface at the outer part of the dolmens; the former is ~1 m deeper than the latter. To represent the age of the inner and outer side of the dolmens, two samples per each dolmen have been collected (JD6In, JD6Out, JD7In, JD7Out) (Figs. 2b and c). Different from these two, the dolmen JD 5 did not show such structure. Instead, an ancient stone coffin was found inside the dolmen (Fig. 2a). From the dolmen JD5, two sediment samples were taken for OSL dating from both sides of the stone structure surrounding the coffin (JD5R and JD5L). In addition to the sediment samples, two ancient human bones, JD5C and JD7C were also collected for radiocarbon dating from the dolmens JD5 and JD7, respectively.

As described earlier, the samples for OSL dating were collected from the topmost fluvial sediments (i.e., immediately underneath the stones). Therefore, it is presumed that the radiation doses absorbed by quartz grains were from both stones and sediments. To take the sample context into account when estimating dose rates, it was necessary to collect stones overlying the sediments,

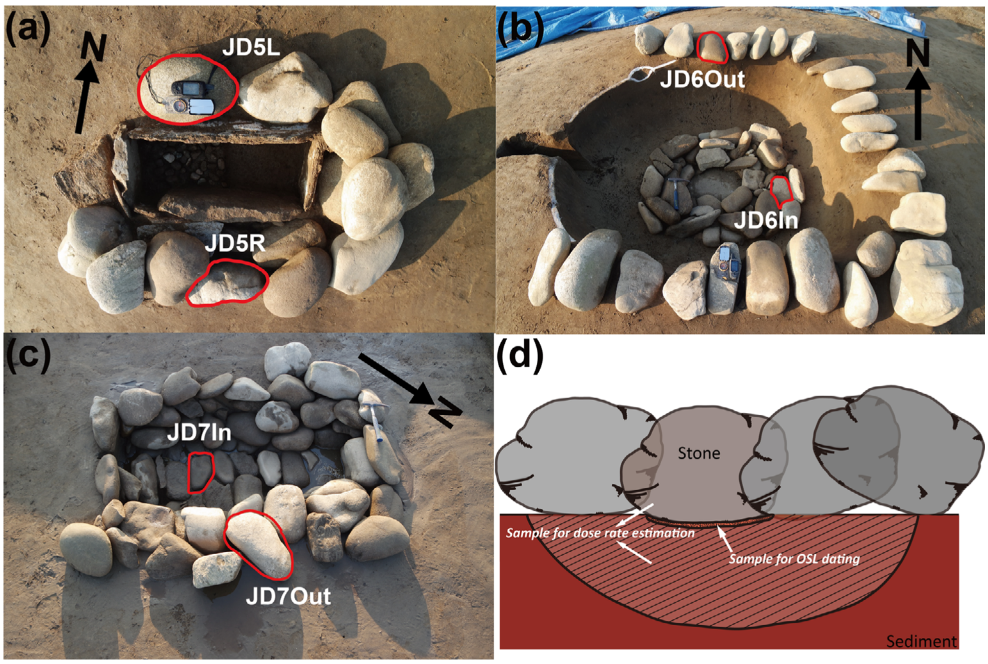

Fig. 2. Six sediment samples were taken from each dolmen (two samples per each). (a–c) The sample locations are marked as solid red lines. (a) There observed a coffin inside the dolmen JD5, together with ancient human bones which were used for radiocarbon dating (lab. Code JD5C). Two samples (JD5L and JD5R) were taken for OSL dating. (b and c) Four OSL samples were also collected from inner and outer parts of the dolmens JD6 (JD6Out and JD6In) and JD7(JD7Out and JD7In). (d) Samples for OSL dating were from the topmost fluvial sediments (down to ~1 cm in depth), immediately underneath the stones making up the dolmens.

 https://doi.org/10.1007/s12303-022-0002-5

from which the samples for OSL dating were taken (Fig. 2d). However, as mentioned, collecting stones from dolmens was strictly prohibited according to Korean Cultural Heritage Protection Law. Alternatively, we collected stones naturally distributed in the archaeological site, which were observed to be of the same type as those making up the dolmens.

3. SAMPLE PREPARATION AND FACILITIES

All the sediment samples were treated in the subdued darkroom to extract quartz grains. Firstly, the samples were wet-sieved to recover size fractions of 90–250 μm. Then, these fractions were treated with 10% HCl and 10% H_2O_2 to remove carbonates and organic matters, respectively, followed by etching with 40% HF (for ~45 min). Finally, quartz grains were prepared by treating the etched samples with 10% HCl to dissolve fluoride precipitates that might have formed during HF etching. The prepared samples were checked for the absence of feldspar contamination by IR (InfraRed) stimulation on the natural and beta-irradiated (~20 Gy) aliquots. Three 8 mm-aliquots for each sample were used for the purity check and, for all the samples, negligible IRSL signals were observed compared with blue-stimulated OSL signals, with the ratios of IRSL to OSL signals being far less than 0.05. This indicates that, through the sample preparation procedure, feldspars were effectively removed.

Quartz OSL signals were measured using a conventional Risø reader (Model TL/OSL-DA-20). Sample irradiation was carried out with a $^{90}Sr/^{90}Y$ beta source delivering ~0.087 ± 0.001 $Gy{\cdot}s^{-1}$ to the sample position. Blue-LEDs (470 nm, FWHM = 20 nm, maximum power density of ~80 $mW{\cdot}cm^{-2}$) was used for optical stimulation of multiple grains. For the stimulation of individual quartz grains, a green laser (532 nm), which is installed in the single grain attachment to the reader, was used. Luminescence signal detection was through a 7.5 mm of Hoya U-340 optical filter.

Equivalent doses (D_e) were estimated using the SAR (Single-Aliquot Regenerative-Dose) procedure (Murray and Wintle, 2000, 2003). For multiple grain measurements, small aliquots (3 mm aliquots), composed of several hundreds of quartz grains, were used. In the SAR procedure, after preheating, the aliquots were stimulated with IR-LED at 50 °C for 100 s prior to every blue stimulation, in order to minimize any detrimental effects from feldspar contamination, if there are any (Roberts, 2007). The OSL signals for D_e estimation were readout for 40 s at 125 °C using Blue-LEDs for optical stimulation. The OSL signals measured in the initial 0.32 s were used for constructing the dose response curves; The signals obtained during immediately following 0.8 s were subtracted as background (Early Background Subtraction; Ballarini et al., 2007).

On the other hand, for D_e estimation using individual quartz grains, IR depletion ratio (Duller, 2003) was used to identify luminescence signals from unwanted feldspar grains that had not been removed by the sample preparation procedure described above; Only the grains that passed through a series of acceptance criteria (i.e., recycling ratio within 10% of unity, recuperation less than 10% of the natural signal intensity, test dose signal more than 3σ above background, IR depletion ratio more than 0.8 etc.) were used for statistical analysis. The OSL signals from individual quartz grains were measured for 2 s at 125 °C, with empty measurements of 0.1 s before and after the green laser stimulation. The spatial non-uniformity of beta dose rates over the single grain disc was corrected for using the program *CorrSGBin*, provided by DTU Physics (Torben et al., 2012). Quartz single grains (180–212 μm in size), which were loaded in 100 holes in each of single grain discs, were used for D_e estimation with the SAR procedure.

Because both the stones and sediments are considered to have contributed to total dose rates, the samples for dose rate estimation were prepared by pulverizing the stones and sediments, and mixing them half and half by weight; We assumed that half of the sphere of radiation is in the stones and the other half in the sediments. The radionuclide concentrations of the mixture samples were then measured using a low-level high resolution gamma spectrometer. Conversion to dose rates used the data presented by Liritzis et al. (2013). The dose rates were modified by using half of the present water contents of the sediment samples, assuming that the water content of the overlying stones are negligible. Cosmic ray contributions were estimated using the method given by Prescott and Hutton (1994).

The bone samples collected from the dolmens JD5 and JD7 (Lab. Codes JD5C and JD7C, respectively) were radiocarbon dated using AMS (Accelerator Mass Spectrometer) installed in Geochron Laboratories, USA. The conventional radiocarbon ages of the samples were calibrated using INTCAL20 (Reimer et al., 2020).

4. RESULTS AND DISCUSSION

4.1. Quartz OSL Signal Properties

In multiple grain aliquot (hereafter, MG) scale, the OSL signals in all the samples from the dolmens selected for this study showed fast decay, the OSL signals being reduced less than 10% of the initial count rates in ~1–3 s after the onset of blue stimulation (Figs. 3a, c, e); This seems to indicate, at least indirectly, that the OSL signals of all the samples are dominated by the fast OSL component, which is the main target signal for dating using the SAR procedure (Wintle and Murray, 2006). The growths of the

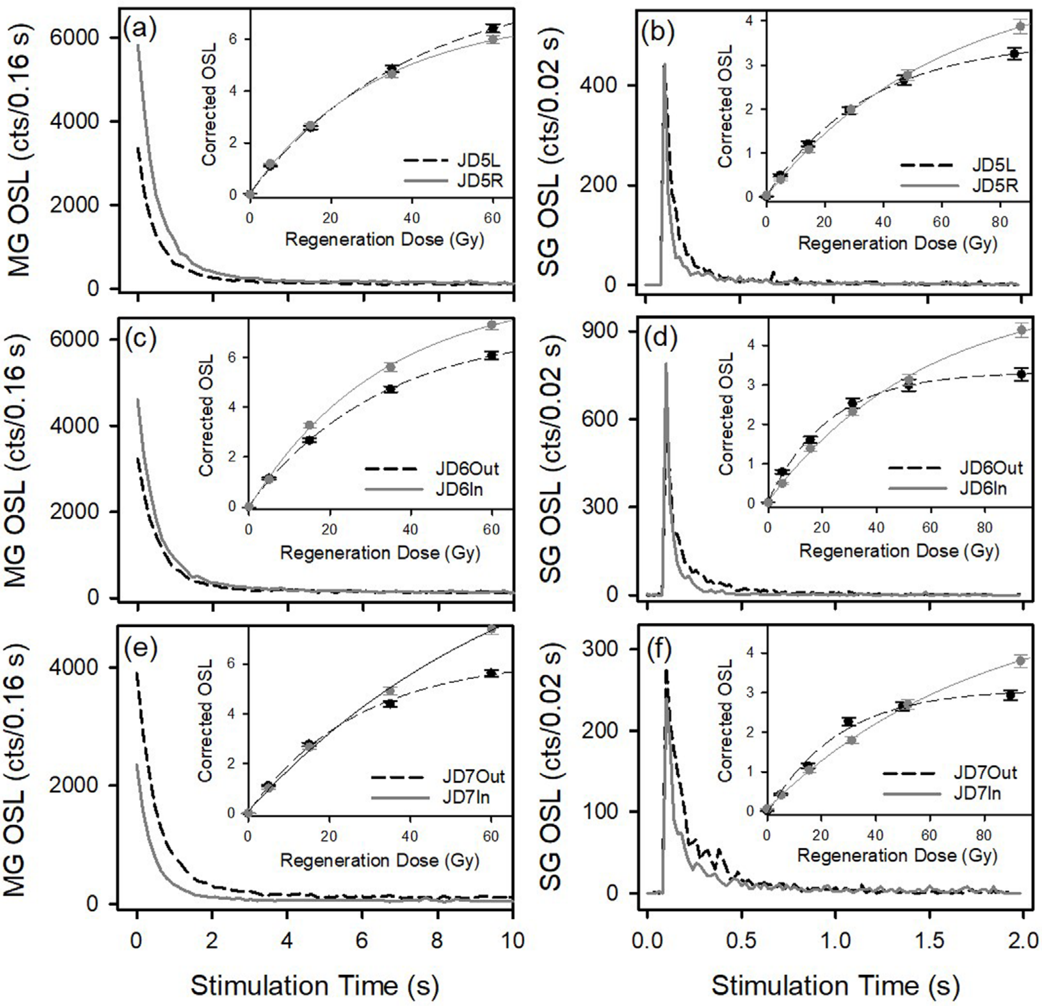

Fig. 3. Representative quartz OSL decay curves of multiple grain aliquots (a, c, e) and individual grains (b, d, f). Dose response curves of each sample are also shown in the insets. (a, c, e) The MG OSL signal intensities were reduced less than 10% of the initial count rates in 1–3 s after the onset of blue stimulation, and the averaged $2D_0$ values of OSL signal growth curves were ~70 Gy for all the samples. (b, d, f) The initial SG OSL count rates were mostly less than 1000 cts/0.02 s.

OSL signals, with increase in regeneration doses, were well defined by single saturating exponential functions (insets to Figs. 3a, c, e). Although there are aliquot-to-aliquot variations, the $2D_0$ values (characteristic doses; Wintle and Murray, 2006) of the samples were ~70 Gy on average.

As for the single grains (hereafter, SG) of quartz, only ~1–2% of the measured grains emitted signals suitable for statistical analysis for deriving the OSL ages. Further, the grains with measurable brightness showed the initial count rates less than 1000 cts/0.02 s, with considerable grain-to-grain variations in $2D_0$ values ranging ~20–300 Gy, as represented in Figures 3b, d, and f. As described in Duller et al. (2000), the variations in OSL signal sensitivity of individual quartz grains were depicted as cumulative light sum (Fig. 4), in which it is observed that the signals emitted from ~20–75% of beta-dosed (15 Gy and 90 Gy) quartz grains contribute 90% of the total OSL intensity of the samples. Particularly, for high-dosed samples (90 Gy), relatively smaller portion of grains (~20–40%) contribute to ~90% of the total OSL intensity, compared with those administered with a low beta dose of 15 Gy (~60–75%). This suggests that the grain-to-grain variations in sensitivity becomes relatively smaller with the decrease in radiation doses absorbed by quartz grains, making the cumulative light sum curves closer to the diagonal (1:1) line.

4.2. Dose Recovery Experiment

To examine the ability of the SAR procedure to recover a known dose given to the samples in the laboratory, five aliquots of each sample were bleached twice with blue-LEDs for 1000 s at room temperature, with an intervening storage for 10000 s (at room temperature) to allow the charges in thermally unstable traps to decay. Following the administration of a laboratory beta

 https://doi.org/10.1007/s12303-022-0002-5

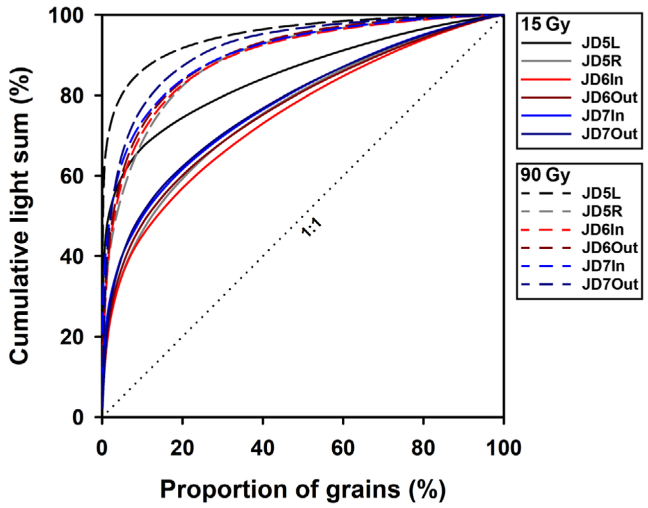

Fig. 4. Cumulative light sum of single grains of quartz. The quartz grains that were irradiated by beta doses of 15 Gy and 90 Gy showed that, ~20–75% of the measured grains contributed to the 90% of the total OSL signal intensities of the samples. This also revealed that the grain-to-grain variations in OSL sensitivity were consistently less for the high-dosed samples (90 Gy) than those with low beta dose of 15 Gy.

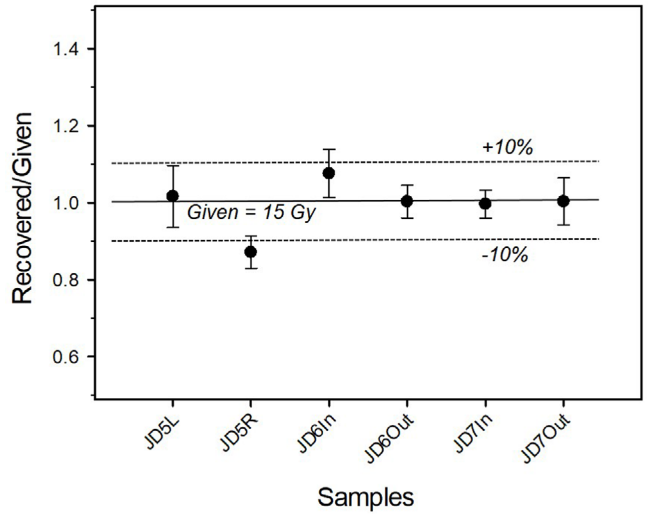

Fig. 5. Dose recovery results using the SAR procedure with the preheat combination of 240 °C for 10 s and 220 °C for 0 s for the main and the test dose measurements, respectively. For all the samples, the laboratory dose (given dose) of 15 Gy were all recovered with the measured to given dose ratios being within 10% of unity.

dose of 15 Gy (given dose) to the bleached aliquots, the SAR procedure, described in section 3. SAMPLE PREPARATION and FACILITIES, was applied to recover the given dose. As shown in Figure 5, for all the samples, the artificial dose of 15 Gy was well recovered using the SAR procedure, with the measured to given dose ratios within 10% of unity; Although the dose given to the sample JD5R seemed to be underestimated by ~10% (measured to given dose ratio: 0.87 ± 0.04), considering the uncertainty, it is regarded as acceptable in this study. Based on the dose recovery experiment, the preheat combination of 240 °C for 10 s for main regeneration dose measurements, and 220 °C for 0 s for test dose measurements was used for both MG and SG OSL dating.

4.3. Radiocarbon Ages in Jungdo

Before discussing the OSL ages, it should be noted here that there are a considerable number of radiocarbon ages that have been reported in the archaeological sites in Jungdo (Gangwon Research Institute of Cultural Heritage, 2013; Hangang Institute of Cultural Heritage, 2013; Gangwon Research Institute of Archaeological and Cultural Properties, 2014), which can be regarded as independent age controls for the OSL ages obtained in this study.

As represented in Figure 6, ~92% of the previously reported radiocarbon ages on charcoals and organic-rich sediments, which are related to ancient human habitation (or activity) in Jungdo, are in the range of 3400–1600 cal yr BP. This age span covers the Bronze and the early Iron Age of Korean peninsula.

Two bone samples collected from the dolmens JD5 and JD7 (lab codes JD5C and JD7C, respectively) were radiocarbon dated in this study, and we obtained radiocarbon ages of 1174–923 cal yr BP for JD5C and 2119–1750 cal yr BP for JD7C. While the age of JD7C is consistent with the existing data, that of JD5C appears to be too young (Fig. 6), compared with the majority of

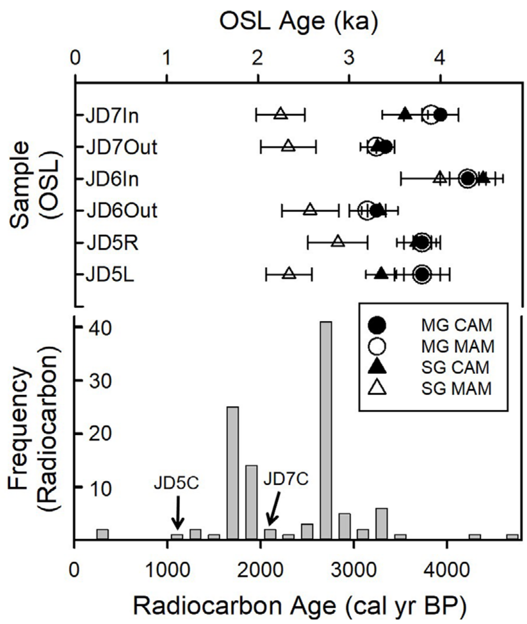

Fig. 6. Multiple and single grain OSL ages of the samples, based on age models CAM and MAM-3. The distribution of radiocarbon ages (calibrated by INTCAL20), previously reported and analysed in this study (JD5C and JD7C), are also presented as histogram. Note that the uncertainties of the OSL ages are depicted in 1σ level.

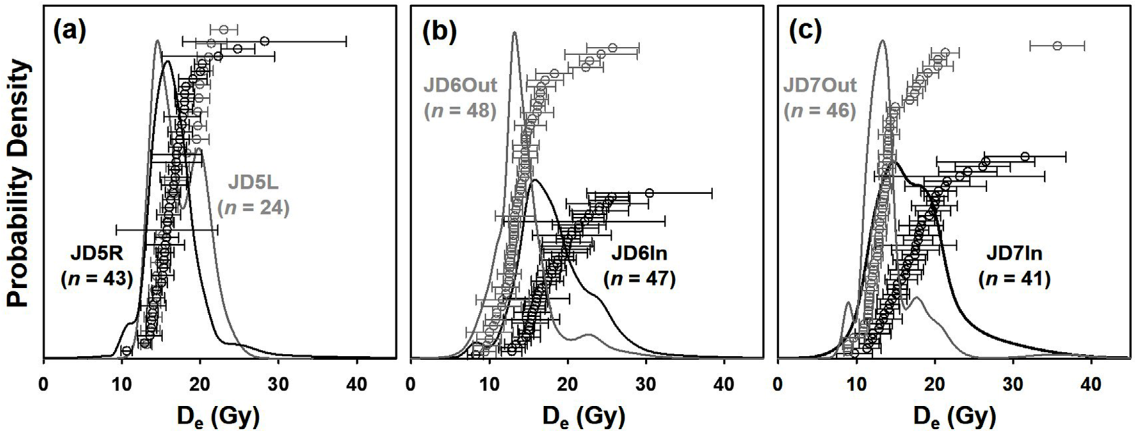

Fig. 7. MG D_e distribution of the samples (a) JD5L and JD5R, (b) JD6Out and JD6In, and (c) JD7Out and JD7In. (a) The samples JD5L and JD5R showed similar D_e distributions. (b and c) However, the D_e values of the samples JD6In and JD7In are generally higher and more normally distributed than those collected from the outer parts of each dolmen (JD6Out and JD7Out).

the previously reported radiocarbon ages in Jungdo. Although we did not examine the causes of this exceptionally young radiocarbon age of the sample JD5C in more detail, it may be attributed to the contamination by young carbon component.

4.4. Multiple-grain Aliquot Ages

For MG-OSL dating, 24–48 aliquots per sample were used. As represented in Figure 7, the MG D_e distribution of two samples collected from the dolmen JD5 (JD5R and JD5L) were similar. On the other hand, samples taken from the inner parts of the dolmens JD6 and JD7 (JD6In and JD7In; refer to the section 2. STUDY AREA and SAMPLE DETAILS) showed higher and more normally distributed D_e values than those from the outer parts of each dolmen (JD6Out and JD7Out). Particularly, the weighted skewness (c) of the samples JD6Out and JD7Out are 1.00 and 1.75, respectively, both of which are higher than $2\sigma_c$ values (significance value for skewness, $\sigma_c = \sqrt{6/n}$, n = number of aliquots) of each sample (i.e., $c > 2\sigma_c$). This led us to the application of MAM-3 (three parameters minimum age model) as the most appropriate age model for these two samples according to the procedure proposed by Bailey and Arnold (2006). This procedure suggested that CAM (central age model) should be the most suitable age model for other four samples; However, it should be noted here that the procedure by Bailey and Arnold (2006) was originally proposed for the analysis of single grain data.

The calculation of CAM and MAM-3 D_e values used R package '*Luminescence*' (v. 0.9.13), developed by *R Luminescence Developer Team* (Kreutzer et al., 2012). The MG CAM ages of the samples JD5L and JD5R are identical to each other with the ages of 3.8 ± 0.2 ka and 3.8 ± 0.1 ka, respectively (Table 1, Fig. 6). The MG CAM ages of the samples JD6Out and JD7Out, both of which were collected from the outer parts of the dolmens JD6 and JD7, were 3.3 ± 0.1 ka and 3.4 ± 0.1 ka. These ages are younger than the inner counterparts JD6In and JD7In, the MG CAM

Table 1. MG equivalent doses, dosimetry and quartz OSL ages

Sample	Water Content (wt%)[a]	Dry beta (Gy·ka^{-1})[b]	Dry gamma (Gy·ka^{-1})[b]	Wet total Dose rate (Gy·ka^{-1})[c]	CAM			MAM-3		n[e]
					D_e (Gy)	OD (%)	Age (ka)[c]	D_e (Gy)	Age (ka)[d]	
JD5L	8	2.79 ± 0.11	1.88 ± 0.04	4.41 ± 0.11	16.9 ± 0.6	15 ± 3	3.8 ± 0.2	17.0 ± 1.1	3.8 ± 0.3	24
JD5R	8	2.73 ± 0.11	1.78 ± 0.03	4.25 ± 0.10	16.2 ± 0.4	13 ± 2	3.8 ± 0.1	16.2 ± 0.7	3.8 ± 0.2	43
JD6Out	7	2.72 ± 0.10	1.77 ± 0.03	4.26 ± 0.10	14.2 ± 0.4	16 ± 2	3.3 ± 0.1	13.8 ± 0.8	3.2 ± 0.2	48
JD6In	9	2.71 ± 0.10	1.70 ± 0.03	4.12 ± 0.10	17.7 ± 0.6	18 ± 3	4.3 ± 0.2	17.7 ± 1.1	4.3 ± 0.3	47
JD7Out	10	2.65 ± 0.10	1.75 ± 0.03	4.05 ± 0.10	13.8 ± 0.5	22 ± 2	3.4 ± 0.1	13.2 ± 0.5	3.3 ± 0.1	46
JD7In	10	2.68 ± 0.10	1.84 ± 0.04	4.16 ± 0.10	16.7 ± 0.6	18 ± 3	4.0 ± 0.2	16.4 ± 1.3	3.9 ± 0.3	41

[a]Present water content.
[b]Data from high-resolution low level gamma spectrometer were converted to infinite matrix dose rates using the conversion factors given in Liritzis et al. (2013).
[c]Contributions from cosmic rays were included using the equations given by Prescott and Hutton (1994).
[d]Ages in the shaded areas are those obtained using the age models chosen according to the procedure suggested by Bailey and Arnold (2006).
[e]Number of aliquots used for statistical analysis.

 https://doi.org/10.1007/s12303-022-0002-5

ages of which are 4.3 ± 0.2 ka and 4.0 ± 0.2 ka, respectively.

When estimating MAM-3 D_e, it is important to make the most reasonable assumption on *sigma b* as this value affects the final MAM-3 D_e estimation. The averaged overdispersion (OD) derived using the CAM model applied to six samples (i.e., 30 multiple grain aliquots) in dose recovery experiments, described in section 4.2., was 8.8%. By quadratically summing this with an assumed extrinsic uncertainty of 15% (De Jong, 2019), the *sigma*

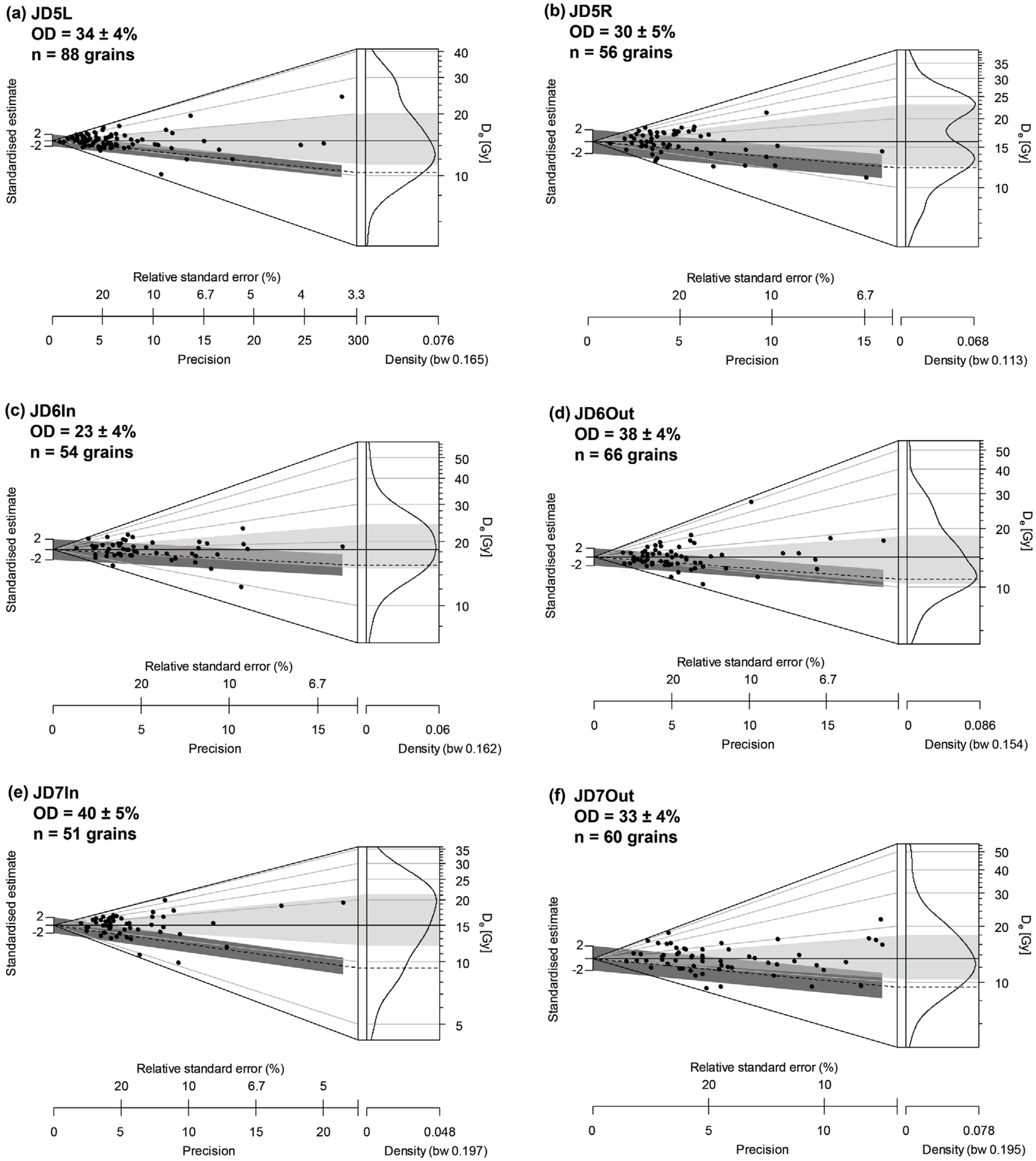

Fig. 8. Abanico plots representing the SG D_e distributions of the samples. The CAM D_e values are indicated by solid lines with 2 sigma bands (pale grey) while MAM-3 D_e values by dotted lines and dark grey 2 sigma bands.

b value of 0.17 was used for calculating the MAM-3 ages of the samples. The MAM-3 ages of all the samples, however, are almost indistinguishable to the CAM ages (Table 1, Fig. 6). As can be seen in Figure 6, both CAM and MAM-3 ages of all the samples, based on multiple grain aliquots, appear to be older than the radiocarbon ages reported in this and previous studies. This may be attributed either to the incorporation of older grains into the samples during sampling at the top ~1 cm of the sediment surface (refer to the section 2) or to the presence of incompletely bleached grains when constructing the dolmens. The older ages (both CAM and MAM-3 ages) of the samples from the inner parts of the dolmens (JD6In and JD7In), compared with those from the outer parts (JD6Out and JD7Out), appear to support the latter scenario; This is further discussed in the following section. To examine the causes of the overestimated MG OSL ages in more detail, we carried out SG dating of the samples.

4.5. Single Grain Ages

The procedure of Bailey and Arnold (2006) applied to SG data suggested the same age models as MG (Tables 1 and 2). That is, CAM was predicted as the most appropriate age model for the samples JD5R, JD6In and JD7In, whereas MAM-3 for the samples JD6Out and JD7Out; As shown in Figure 8, the SG D_e distributions of the samples JD5R, JD6In and JD7In showed the weighted skewness less than $2\sigma_c$ values (i.e., $c < 2\sigma_c$) and the overdispersions less than 50%. On the other hand, for the samples JD6Out and JD7Out, the weighted skewness was higher than $2\sigma_c$ values, resulting in MAM-3 as the output of the age model-decision procedure. According to the procedure, 'Lowest 5%' (L5%) model (e.g., Olley et al., 1998; Thomsen et al., 2016) was recommended for the sample JD5L, because the weighted skewness (0.57) of the SG D_e distribution was slightly higher than $2\sigma_c$ (0.52) and the weighted kurtosis (0.24) lower than σ_k (0.52; significance value for kurtosis, $\sigma_k = \sqrt{24/n}$, n = number of grains), with overdispersion value over 10%.

The SG CAM ages of the samples JD5R, JD6In and JD7In (4.5–3.6 ka) were in the similar range to MG CAM ages (4.3–3.8 ka; Tables 1 and 2, Fig. 6), all of which are still older than the previous radiocarbon ages. To the contrary, the age model MAM-3 applied to the samples JD6Out and JD7Out yielded the SG ages of 2.6 ± 0.3 ka and 2.3 ± 0.3 ka, respectively; Dose recovery experiments on single grains were not carried out in this study, thus the intrinsic uncertainty of the single grain D_e values of the samples could not be assessed. Therefore, when estimating MAM-3 D_e values of the samples investigated here, *sigma b* value of 0.2 was assumed as in many previous studies (e.g., Arnold and Roberts, 2009; Nimick et al., 2016; Sauer et al., 2016; Kappler et al., 2018, Moreno et al., 2021). The MAM-3 ages of the samples JD6Out and JD7Out are consistent with each other and the existing radiocarbon ages. Note that the SG MAM-3 ages of other two samples (JD5R and JD7In), for which CAM was predicted by the age model-decision procedure, are respectively 2.9 ± 0.3 ka and 2.2 ± 0.3 ka, also comparable with those of the samples JD6Out, JD7Out and radiocarbon ages (Table 2, Fig. 6). Although not shown in Table 2 and Figure 6, the application of SG L5% model to the sample JD5L yielded the D_e value of 7.3 ± 2.4 Gy, resulting in the age of 1.7 ± 0.5 ka. However, it is difficult to give statistical credence to this age because only 5 grains (lowest 5% of 88 grains measured) were used to derive the L5% D_e estimate. Thus, this age is not further discussed in this study. Instead, the SG MAM-3 age of the sample JD5L is 2.3 ± 0.3 ka, which is in good agreement with that of the sample from the same dolmen JD5 (JD5R; 2.9 ± 0.3 ka). The radiocarbon age on the human bone excavated from the dolmen JD5 (1174–923 cal yr BP), discussed in section 4.3. Radiocarbon Ages in Jungdo, is still younger than the SG MAM-3 ages of the samples JD5R and JD5L, suggesting that the radiocarbon age of JD5C is presumably underestimated one by young carbon component or else.

Based on the single grain ages, it is considered that, although the age model-decision procedure predicted CAM for half of the samples, the final age estimates obtained by MAM-3 for all the samples are most comparable with the radiocarbon ages from archaeological sites in Jungdo, and also self-consistent showing

Table 2. SG equivalent doses, dosimetry and quartz OSL ages

Sample	Wet total Dose rate (Gy·ka^{-1})[a]	CAM			MAM-3		n/N[c]
		D_e (Gy)	OD (%)	Age (ka)[b]	D_e (Gy)	Age (ka)[b]	
JD5L	4.41 ± 0.11	14.8 ± 0.6	34 ± 4	3.4 ± 0.2	10.3 ± 1.1	2.3 ± 0.3	88/6300
JD5R	4.25 ± 0.10	15.9 ± 0.8	30 ± 5	3.7 ± 0.2	12.2 ± 1.4	2.9 ± 0.3	56/5000
JD6Out	4.26 ± 0.10	14.2 ± 0.8	38 ± 4	3.3 ± 0.2	11.0 ± 1.3	2.6 ± 0.3	66/5300
JD6In	4.12 ± 0.10	18.4 ± 0.8	23 ± 4	4.5 ± 0.2	16.5 ± 1.7	4.0 ± 0.4	54/4600
JD7Out	4.05 ± 0.10	13.4 ± 0.7	33 ± 4	3.3 ± 0.2	9.5 ± 1.2	2.3 ± 0.3	60/4700
JD7In	4.16 ± 0.10	15.0 ± 1.0	40 ± 5	3.6 ± 0.2	9.4 ± 1.1	2.2 ± 0.3	51/5900

[a]Wet total dose rates are the same as those used in the age calculation based on multiple grain aliquots.
[b]Ages in the shaded areas are those obtained using the age models chosen according to the procedure suggested by Bailey and Arnold (2006).
[c]n denotes the number of grains used for statistical analysis, and N is the total number of measured grains.

https://doi.org/10.1007/s12303-022-0002-5

the SG MAM-3 ages in the range of 2.9–2.2 ka (Table 2, Fig. 6). The older SG CAM ages, compared with those using the age model MAM-3, are presumably attributed to the incorporation of incompletely grains into the samples while sampling, as discussed in the previous section (section 4.4. Multiple-Grain Aliquot Ages).

The SG MAM-3 age of the sample JD6In is, however, 4.0 ± 0.4 ka, still higher than the MAM-3 ages of other samples; The age of 4.0 ± 0.4 ka is even older than the previously reported radiocarbon ages. From field observation (see Fig. 2), it is inferred that, when constructing the dolmens JD6 and JD7, the sediments in the inner parts were dug out more than ~1 m deep from the exposed ground surface and then stones were stacked in the pit, whereas the stones at the outer parts were directly put on the surface of the fluvial sediments. Thus, the quartz grains underneath the stones stacked in the pit are considered to have less chances to be exposed to sunlight for effective bleaching of OSL signals than those from the outer parts. It seems that this effect is observed also both in the MG CAM and MG MAM-3 ages, which are older for the samples from the inner parts (JD6In and JD7In) than the corresponding outer parts of dolmens (JD6Out and JD7Out). The age difference between the samples from the inner and outer parts of the dolmens are even observed in the SG CAM ages. For the sample JD7In, by applying the MAM-3, we could obtain the age indistinguishable from that of JD7Out (Table 2; 2.2 ± 0.3 ka and 2.3 ± 0.3 ka for the samples JD7In and JD7Out, respectively) and these ages are further in good agreement with the radiocarbon ages of a bone sample collected from the dolmen JD7 (JD7C; 2119–1750 cal yr BP). We could not observe such improvement in age estimation by applying MAM-3 to the sample JD6In. Although we presume that this may be due to more unfavourable conditions for the OSL signal bleaching of quartz grains inside the pit of the dolmen JD6 than those of JD7, at this stage, it is difficult to figure out the causes of the older SG MAM-3 ages of the sample JD6In. Therefore, the sample JD6In was not further considered in the interpretation of the construction timing of the dolmens in Jungdo.

5. CONCLUSIONS

In this paper, we investigated the multiple and single grain quartz OSL dating on the samples collected from three dolmens in Jungdo. The samples from fluvial sediments underneath the stones making up the dolmens showed almost identical multiple grain CAM and MAM-3 ages, ranging 4.3–3.3 ka and 4.3–3.2 ka, respectively. These ages are observed to be older than previous radiocarbon ages on samples from archaeological sites in Jungdo. The CAM applied to the single grain quartz resulted in similar age range to both multiple grain CAM and MAM-3 ages. Particularly, for the samples collected from the inner parts of the dolmens, the OSL ages, based on multiple grain CAM, MAM-3 and single grain CAM, were older than those from the outer parts. However, by applying MAM-3 model to single quartz grains, we could obtain OSL age estimates which are consistent with radiocarbon ages, except the sample JD6In. Further, for one site (JD7), the single grain ages of the samples from inner and outer parts of dolmen became in good agreement with each other by applying the age model MAM-3, which indicates that, when constructing dolmens in Jungdo, the sediments in the inner part of the dolmen were less bleached by sunlight than those in the outer part. The single grain MAM-3 ages of the samples reveal that the dolmens investigated here were built during late Bronze to early Iron age (2.9–2.2 ka), suggesting that Jungdo has been the place either for burial plots or habitation of the ancient humans up to early Iron Age in the central part of Korean peninsula.

Our results also suggest that, in order to OSL date dolmens or any megalithic archaeological remains using the sediments underneath the stones, minimum age model applied to single grains appears to be more promising than other age models for multiple grains.

ACKNOWLEDGMENTS

This work was supported by a Korea Basic Science Institute grant (C230120) and partly by a grant from National Research Foundation of Korea (PG2021154).

REFERENCES

Arnold, L.J. and Roberts, R.G., 2009, Stochastic modelling of multi-grain equivalent dose (D_e) distributions: implications for OSL dating of sediment mixtures. Quaternary Geochronology, 4, 204–230.

Athanassas, C.D., Rollefson, G.O., Kadereit, A., Kennedy, D., Theodorakopoulou, K., Rowan, Y.M., and Wasse, A., 2015, Optically stimulated luminescence (OSL) dating and spatial analysis of geometric lines in the Northern Arabian Desert. Journal of Archaeological Science, 64, 1–11.

Athanassas, C.D., Sanjuán, L.G., Stamoulis, K., Romero, R.L., Carinou, E., and Curado, R.A., 2017, Optically stimulated luminescence (OSL) dating of an enigmatic, megalithic-like, subterranean structure in Carmona (Seville, Spain). Journal of Archaeological Science: Report, 16, 240–247.

Bae, C.J. and Kim, B., 2015, Korea prehistory: current perspectives. Asian Perspectives, 54, 1–10.

Bailey, R.M. and Arnold, L.J., 2006, Statistical modelling of single grain quartz D_e distributions and an assessment of procedures for estimating burial dose. Quaternary Science Reviews, 25, 2475–2502.

Ballarini, M., Wallinga, J., Wintle, A.G., and Bos, A.J.J., 2007, A modified SAR protocol for optical dating of individual grains from young quartz samples. Radiation Measurements, 42, 360–369.

Chapot, M.S., Sohbati, R., Murray, A.S., Pederson, J.L., and Rittenour, T.M., 2012, Constraining the age of rock art by dating a rockfall

event using sediment and rock-surface luminescence dating techniques. Quaternary Geochronology, 13, 18–25.
De Jong, C., 2019, Testing the suitability of luminescence dating on Quaternary badland deposits, Kula, Turkey. M.Sc. Thesis, Wageningen University & Research, Wageningen, 48 p.
Duller, G.A.T., 2003, Distinguishing quartz and feldspar in single grain luminescence measurements. Radiation Measurements, 37, 161–165.
Duller, G.A.T., Bøtter-Jensen, L., and Murray, A.S., 2000, Optical dating of single sand-sized grains of quartz: sources of variability. Radiation Measurements, 32, 453–457.
Galbraith, R.F., Roberts, R.G., Laslett, G.M., Yoshida, H., and Olley, J.M., 1999, Optical dating of single and multiple grains of quartz from Jinmium rock shelter, northern Australia: Part I. Experimental design and statistical models. Archaeometry, 41, 339–364.
Gangwon Research Institute of Archaeological and Cultural Properties, 2014, The excavation report on Jungdo-dong site, Chuncheon. Research Report, 30, Wonju, 349 p.
Gangwon Research Institute of Cultural Heritage, 2013, The excavation report on Jungdo-dong site, Chuncheon. Research Report, 127, Chuncheon, 464 p.
Greilich, S., Glasmacher, U.A., and Wagner, G.A., 2005, Optical dating of granitic stone surfaces. Archaeometry, 47, 645–665.
Hangang Institute of Cultural Heritage, 2013, Jungdo-dong site, Chuncheon. Research Report, 38, Seoul, 465 p.
Kang, B.W., 2010, An examination of chronology, ethnic group, and social ranking based on mortuary data from central Korea. Asian Perspectives, 49, 180–204.
Kappler, C., Kaiser, K., Tanski, P., Klos, F., Füllinf, A., Mrotzek, A., Sommer, M., and Bens, O., 2018, Stratigraphy and age of colluvial deposits indicating Late Holocene soil erosion in northern Germany. Catena, 170, 224–245.
Kim, B., 2015, Socioeconomic development in the Bronze Age: archaeological understanding of the transition from the Early to Middle Bronze Age, South Korea. Asian Perspectives, 541, 144–184.
Ko, I., 2009, New perspectives in Korean funerary archaeology. The Review of Korean Studies, 12, 101–121.
Kostov, R.I., 2008, Geological and mineralogical background of the megalithic and rock-cut sites in Bulgraia and some other European countries. Proceedings of the International Conference on Geoarchaeology and Archaeomineralogy, Sofia, Oct. 29–30, p. 163–168.
Kreutzer, S., Schmidt, C., Fuchs, M.C., Dietze, M., Fischer, M., and Fuchs, M., 2012, Introducing an R package for luminescence dating analysis. Ancient TL, 30, 1–8.
Laporte, L., Bocoum, H., Cros, J.P., Delvoye, A., Bernard, R., Diallo, M., Diop, M., Kane, A., Dattois, V., Lejay, M., Bertin, F., and Quesnel, L., 2012, Megalithic monumentality in Africa: from graves to stone circles at Wanar, Sengegal. Antiquity, 86, 409–427.
Liritzis, I., Stamoulis, K., Papachristodoulou, C., and Ioannides, K., 2013, A re-evaluation of radiation dose-rate conversion factors. Mediterranean Archaeology and Archaeometry, 13, 1–15.
Moreno, D., Gutiérrez, F., del Val, M., Carbonel, D., Jiménez, F., Alonso, M.J., Martínez-Pillado, V., Guzmán, O., López, G.I., and Martínez, D., 2021, A multi-method dating approach to reassess the geochronology of faulted Quaternary deposits in the central sector of the Iberian Chain (NE Spain). Quaternary Geochronology, 65, 101185.
Murray, A.S. and Wintle, A.G., 2000, Luminescence dating of quartz using an improved single-aliquot regenerative-dose protocol. Radiation Measurements, 32, 57–73.
Murray, A.S. and Wintle, A.G., 2003, The single aliquot regenerative dose protocol: potential for improvements in reliability. Radiation Measurements, 37, 377–381.
Nelson, S.M., 2014, Megalithic monuments in Korea. In: Selin, H. (ed.) Encyclopaedia of the History of Science, Technology, and Medicine in Non-Western Cultures. Springer, Dordrecht. https://doi.org/10.1007/978-94-007-3934-5_8772-2
Nesterkina, A.L., Solovieva, E.A., Tabarev, A.V., and Ivanova, D.A., 2017, The megaliths of Korea and Japan: an analysis of origins and functions. Archaeology, Ethnology and Anthropology of Eurasia, 45, 106–114.
Nimick, D.A., McGrath, D., Mahan, S.A., Friesen, B.A., and Leidich, J., 2016, Latest Pleistocene and Holocene glacial events in the Colonia valley, northern Patagonia Icefield, South Chile. Journal of Quaternary Science, 31, 551–564.
Olley, J.M., Caitcheon, G., and Murray, A.S., 1998, The distribution of apparent dose as determined by optically stimulated luminescence in small aliquots of fluvial quartz: implications for dating young sediments. Quaternary Science Reviews, 17, 1033–1040.
Prescott, J.R. and Hutton, J.T., 1994, Cosmic ray contribution to dose rates for luminescence and ESR dating: large depths and long-term time variation. Radiation Measurements, 23, 497–500.
Reimer, P.J., Austin, W.E.N., Bard, E., Bayliss, A., Blackwell, P.G., Ramsey, C.B., Butzin, M., Cheng, H., Edwards, R.L., Friedrich, M., Grootes, P.M., Guilderson, T.P., Hajdas, I., Heaton, T.J., Hogg, A.G., Hughen, K.A., Kromer, B., Manning, S.W., Muscheler, R., Palmer, J.G., Pearson, C., van der Plicht, J., Reimer, R.W., Richards, D.A., Scott, E.M., Southon, J.R., Turney, C.S.M., Wacker, L., Adolphi, F., Büntgen, U., Capano, M., Fahrni, S.M., Fogtmann-Schulz, A., Friedrich, R., Köhler, P., Kudsk, S., Miyake, F., Olsen, J., Reinig, F., Sakamoto, M., Sookdeo, A., and Talamo, S., 2020, The INTCAL20 northern hemisphere radiocarbon age calibration curve (0–55 CAL kBP). Radiocarbon, 62, 725–757.
Rhee, S.N. and Choi, M.L., 1992, Emergence of complex society in prehistoric Korea. Journal of World Prehistory, 6, 51–95.
Roberts, H.M., 2007, Assessing the effectiveness of the double-SAR protocol in isolating a luminescence signal dominated by quartz. Radiation Measurements, 42, 1627–1636.
Sauer, D., Kadereit, A., Kühn, P., Kösel, M., Miller, C.E., Shinonaga, T., Kreutzer, S., Hermann, L., Fleck, W., Starkovich, B.M., and Stahr, K., 2016, The loess-palaesol sequence of Datthausen, SW Germany: characteristics, chronology, and implications for the use of Lohne Soil as a marker soil. Catena, 146, 10–29.
Sharon, G., Barash, A., Eisenberg-Degen, D., Grosman, L., Oron, M., and Berger, U., 2017, Monumental megalithic burial and rock art tell a new story about the Levant Intermediate Bronze "Dark Ages". PloS One, 12, e0172969. https://doi.org/10.1371/journal.pone.0172969
Thomsen, K.J., Murray, A.S., Buylaert, J.P., Jain, M., Hansen, J.H., and Aubry, T., 2016, Testing single-grain quartz OSL methods using sediment samples with independent age control from the Bordes-Fitte rockshelter (Roches d'Abilly site, central France). Quaternary Geochronology, 31, 77–96.

Torben, L., Jain, M., Thomsen, K.J., Murray, A.S., and Buylaert, J.-P., 2012, New luminescence measurement facilities in retrospective dosimetry. Radiation Measurements, 47, 803–808.

Wintle, A.G. and Murray, A.S., 2006, A review of quartz optically stimulated luminescence characteristics and their relevance in single-aliquot regeneration dating protocols. Radiation Measurements, 41, 369–391.

Wright, J., 2007, Organizational principles of Khirigsuur monuments in the lower Egiin Gol valley, Mongolia. Journal of Anthropological Archaeology, 26, 350–365.